Journal of Electrical and Electronic Engineering
2022; 10(5): 184-198
http://www.sciencepublishinggroup.com/j/jeee
doi: 10.11648/j.jeee.20221005.12
ISSN: 2329-1613 (Print); ISSN: 2329-1605 (Online)

Lattice Predictors for a Stagger-Period Sequence: Their Theory and Application

Xubao Zhang[1, 2]

[1]Electronic Engineering Department, Xi'an Electronic Science and Technology University, Xi'an, China

[2]Research & Development, Unitron Hearing, Kitchener, Canada

Email address:
xbzwdl@yahoo.com

To cite this article:
Xubao Zhang. Lattice Predictors for a Stagger-Period Sequence: Their Theory and Application. *Journal of Electrical and Electronic Engineering*. Vol. 10, No. 5, 2022, pp. 184-198. doi: 10.11648/j.jeee.20221005.12

Received: August 23, 2022; **Accepted**: September 13, 2022; **Published**: September 21, 2022

Abstract: This paper proposes a new structure of lattice predictors, which applies to a stagger-period sequence. To deal with the sequence's time-varying periods, the stagger-period lattice predictor has a linear time-variant processing structure, whose reflection coefficients and delay units need to match the input sequence periods for optimality. The staggered lattice predictor's operation is relatively complex, of ∑M forward and backward reflection coefficients, M its order; and a uniform-period lattice predictor consists of M forward and backward coefficients. Based on Burg's uniform-period lattice algorithm, we propose the staggered Forward and Backward Error Minimum algorithm to determine this predictor's reflection coefficients and prove its optimality in the sense of minimum mean square error. By means of staggered forward and backward transversal predictors, we also propose the staggered Levinson-Durbin relations and prove it holds in the Appendix; these relations play an important role in researching the staggered lattice predictor. For practical application, we present a corresponding reflection coefficient estimation, the staggered Arithmetic Mean method, which substitutes for the ensemble mean with the limited-sample mean, and minimizes the estimate's variance in the least square error sense. Through many computer simulations, we investigate convergence performance and learning characteristic of this type of predictor with three observation goals: the reflection coefficient, prediction error, and frequency response; the investigations reveal relationships between the convergence performance, learning characteristic and the balance factor, length of averaging window. In order to apply the staggered lattice predictor to an actual field, we illustrate a moving target indicator for Doppler radar with a stagger-period pulse emission and pulse compression waveform technology. Our simulation tests demonstrate that the staggered block lattice filter with essential artificial intelligence (AI) can efficiently detect weak targets submerged in the stationary and nonstationary clutters. The AI includes five heuristic strategies based on radar professionals' knowledge to preserve targets and reject false alarms.

Keywords: Lattice Predictor, Stagger-Period Signal Processing, Lattice Prediction Convergence, Moving Target Indicator, Artificial Intelligence

1. Introduction

For about five decades, many researchers studied lattice prediction theories and applied them to many fields, such as speech analysis and identification, geophysical exploration, spectrum estimation, adaptive clutter suppression, etc. [1-7]. A lattice predictor has prominent advantages over a transversal predictor using matrix inversion solution: independent, cascaded modular operation, low sensitivity of coefficient quantization, and less complex computation. They are extensively valued in system identification and adaptive filtering. Gediminas Simkus et al. proposed a low latency audio coding scheme composed of differential pulse code modulation and block companded (compress to expand) quantization [4]. Its encoder and decoder contain the same lattice predictors of finite impulse response (FIR) form, using the plain gradient adaptive lattice algorithm of low computational complexity. The prediction error signal is transmitted from the encoder output to the decoder input and the reconstructed signals are the same. This scheme introduced a small delay and improved the perceptual audio quality significantly. Kensaku Fujii et al. proposed a method to estimate reflection coefficients of a lattice filter, which

decreases number of the divisions to unity when the lattice order is high [5]. The method produces the least prediction errors under a condition that the backward reflection coefficients are replicas of the forward reflection coefficients. Through the theoretical derivation of differential equation, Rui Zhu et al. proposed a normalized lattice filter with a single pole and single zero structure [6]. It is less complex in computation and can acquire the frequency of a complex, input signal. The computer simulation demonstrated that its convergence rate is faster than the conventional gradient-based adaptive notch filter. B. M. Keel et al. designed a complex lattice filter used for the weather radar to reject ground clutters when observing a dry microburst [7]; they incorporated the square root normalized recursive-least-squares algorithm to estimate the reflection coefficients. The clutter data were acquired from realistic radar returns of an airport; the test results indicated that the clutter was rejected by about 30 dB with little attenuation of the weather signal in the relevant range cells.

The above contributions were based on the uniform-period signal sources. In real-world, there exists a class of stagger-period signals and irregular-interval array signals, which may be deliberately produced or naturally acquired. When the stagger-period signal is predicted or filtered or its spectrum is estimated with the theories and methods of the uniform-period lattice predictor, the resulting performances may seriously decline. To solve such a problem, some scholars have been researching on the related stagger-period signal processing [8-13]. Zhang Xubao proposed the theory of FIR filters for stagger-period sequence, introduced the concepts and the time-variant property of the staggered filters [13]. He described the design principles of stagger-period frequency-selective FIR filters and presented the stagger-period matrix inversion and eigenvalue solutions of signal-noise-ratio maximization. He also introduced the moving target indication /indicator (MTI) filter bank design with optimal improvement factor and the mathematical programming to search for the best stagger-period code.

Referring to philosophies and methods of the uniform-period lattice, based on the criterion of minimum mean square errors (MSE), this paper studies a new lattice structure which applies to predicting the stagger-period sequence, called the stagger-period or staggered lattice predictor. The next section presents the operation principle and properties of the staggered lattice predictor based on staggered transversal predictors. Section 3 studies the optimality theory and reflection coefficient algorithms of this lattice predictor. In section 4, the reflection coefficient estimation methods and convergence performance of this predictor in stationary sequences are presented, tested, and discussed. In section 5, the learning characteristic of this predictor in nonstationary sequences is investigated by different observation goals. In section 6, to demonstrate the applicability in signal detection, we design a staggered block lattice predictor for an MTI, which incorporates essential heuristic strategies, to verify the performance of detecting moving target and rejecting false alarm. The last section summarizes all the stagger-period prediction research and gives several exclusive conclusions. In the Appendix, we prove the stagger-period Levinson-Durbin (L-D) relations. A lattice predictor can be of all-zero or all-pole form. In this paper, we study the former only.

2. Structure of a Stagger-Period Lattice Predictor

2.1. A Uniform-Period Lattice Predictor

Over fifty years ago, Levinson, Durbin, et al. researched an algorithm: recursively updating coefficients of the transversal predictor from low order to high order, instead of matrix inversion operation; later, the efficient algorithm became popular in analytical applications [1]. Based on the L-D algorithm, Itakura and Saito derived a lattice structure with stage-by-stage operation, which is uniquely equivalent to the combination of forward and backward transversal predictors in the sense of equal prediction errors [14]. In the uniform-period case, given a discrete-time complex sequence z (nT), n $\in\{0, 1, \cdots\}$, T is the sampling period, the forward and backward prediction errors of an order M lattice predictor at the stage m are computed, respectively,

$$e_m^f(n)= e_{m-1}^f(n)+R_m^* e_{m-1}^b(n-1),\ m\in\{1, 2, \cdots, M\}, \quad (1)$$

$$e_m^b(n)= e_{m-1}^b(n-1) +R_m e_{m-1}^f(n),\ m\in\{1, 2, \cdots, M\}, \quad (2)$$

$$e_0^f(n)= e_0^b(n)= z\ (nT), \quad (3)$$

where R_m^* and R_m are forward and backward reflection coefficients, respectively, * complex conjugation. The lattice predictor has M forward and backward reflection coefficients. In the analytic sense, both the reflection coefficients meet $|R_m|<1$. From the L-D recursive algorithm, when M forward and backward transversal predictors are given, the equivalent M forward and backward lattice reflection coefficients are determined and vice versa. Thus, if the transversal predictors are optimal in the minimum MSE sense, the resulting lattice predictor is so. The reflection coefficients $\{R_m\}$ can also be determined from other algorithms, e.g., Burg's Harmonic Mean algorithm [15].

However, the uniformed lattice predictor does not apply to a stagger-period sequence since the sequence periods are unmatched by the lattice delay units. Table 1 lists the prediction error powers of a uniformed lattice predictor of order 4 in uniform-period and stagger-period stationary sequences of two models. One model C-MS0 is a single-Gaussian spectrum clutter, its parameters are: power P_g 60 dB (noise 0 dB), frequency F_g 0 Hz, and standard variance D_g 3.6 Hz; another C-MS4 is dual-Gaussian spectrum clutter, C-MS0 mixed with an additional clutter whose parameters are P_w 40 dB, F_w 72 Hz, and D_w 14.4 Hz. The reflection coefficients of the uniformed lattice were analytically obtained from the transversal predictor with minimum MSE and L-D algorithm [1]. In the table, we see that on the 1st data row, the period of uniform-period sequence is 2.78 ms, error powers of the predictor are −50.3 and −36.5 dB in C-MS0 and

CMS4, respectively. However, for a stagger-period sequence, period scale 2.42:2.92:2.62:2.82:3.12 ms, average period 2.78 ms on the 2nd row, the error powers of the predictor are −39.8 and −27.8 dB in C-MS0 and CMS4, respectively, much larger than −50.3 and −36.5 dB; and more error powers on rows three to six indicate the similar degradation. Thus, the performances of the uniformed lattice predictor degrades about 10 dB.

Table 1. *Error powers of a uniform-period lattice predictor with uniform-period and stagger-period sequences.*

Periods of Sequences (ms) T1:T2:T3:T4:T5	Sequence models	
	C-MS0	C-MS4
	(dB)	(dB)
2.78:2.78: 2.78:2.78:2.78	−50.3	−36.5
2.42:2.92:2.62:2.82:3.12	−39.8	−27.8
2.92:2.62:2.82:3.12:2.42	−37.9	−28.8
2.62:2.82:3.12:2.42:2.92	−37.2	−25.4
2.82:3.12:2.42:2.92:2.62	−47.4	−22.5
3.12:2.42:2.92:2.62:2.82	−36.8	−23.9

2.2. A Stagger-Period Lattice Predictor

In the case of stagger-period discrete-time signals, some concepts for prediction study are essential to know at first. Given a discrete-time sequence $z(t_n)$, $n \in \{0, 1, \cdots\}$, when time $\{t_n\}$ meets $t_n - t_{n-1} \neq t_{n+1} - t_n$, the sequence is called the stagger-period sequence. A stagger-period sequence can have infinite stagger periods; in reality, the periods are always finite, denoted by $T_n = t_n - t_{n-1}$, $n \in \{1, 2, \cdots, N_t\}$, N_t is number of the stagger periods. If $\{z(t_n)\}$ has N_t stagger periods and the other periods repeat the N_t periods, its stagger periods are N_t-circular. When $N_t = 1$, it declines to a uniform-period sequence; thus, a uniform-period sequence is a special case of the stagger-period sequences. Figure 1 shows waveforms of a circulating stagger-period complex sequence, $N_t = 5$, the stagger-period scale, T1:T2:T3:T4:T5= 2.42:2.92: 2.62:2.82:3.12 ms.

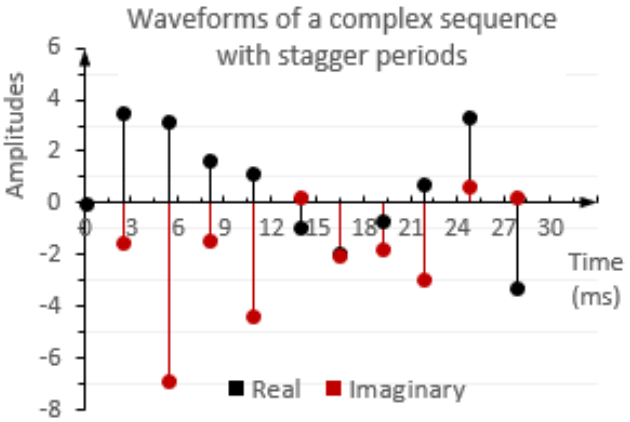

Figure 1. *Waveforms of a stagger-period complex sequence.*

Assuming that a stagger-period sequence $z(t_n)$, $n \in \{0, 1, \cdots\}$, is stationary, its M samples are denoted by a vector $Z^b = [z(t_1), z(t_2), \cdots, z(t_M)]^T$, ^{T} transition. When a transversal predictor of order M predicts $z(t_0)$ and its transversal coefficients are denoted by a vector $H^b = [h^b(t_1), h^b(t_2), \cdots, h^b(t_M)]^T$ as in Figure 2, this predictor is referred to as the stagger-period (or staggered) one-step backward transversal predictor. The prediction error between the input $z(t_0)$ and the predicted value $\hat{z}(t_0)$ is

$$e^b(t_0) = z(t_0) + \hat{z}(t_0) = z(t_0) + H^{b\dagger} Z^b, \quad (4)$$

where † is conjugation transition. When $z(t_0)$ times $h^{b*}(t_0) = 1$ is summed with $\hat{z}(t_0)$ as denoted by the dashed lines in Figure 2, the structure turns into a transversal prediction filter, also a transversal predictor for short. Given that the covariance matrix of stagger-period vector Z^b is M_z^b, whose elements are $E\{z(t_i)z^*(t_j)\}$, $i, j \in \{1, 2, \cdots, M\}$, $E\{\}$ expectation operator, and the covariance vector between Z^b and $z(t_0)$ is R_z^b, whose elements are $E\{z(t_0)z^*(t_i)\}$, $i \in \{1, 2, \cdots, M\}$, the stagger-period Yule-Walker equation can be derived as [13]

$$M_z^b H^b = R_z^b \quad (5)$$

Because M_z^b does not have Toeplitz property, we have to prove that the solution of (5), H^b, results in the minimum $E\{|e^b(t_0)|^2\}$. By the orthogonality theory [1], it was proved that (5) holds for the stagger-period sequence; here we omit the proof due to its similarity to the uniform-period case.

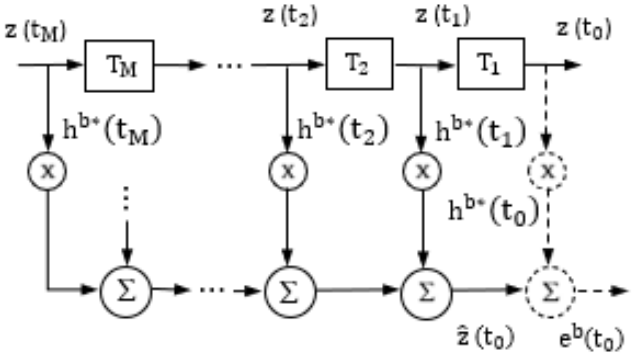

Figure 2. *A stagger-period one-step backward transversal predictor of order M.*

Given that M_z^f is the covariance matrix of stagger-period vector $Z^f = [z(t_0), z(t_1), \cdots, z(t_{M-1})]^T$ and R_z^f is the covariance vector between Z^f and the predicted $z(t_M)$, in the same way above, we proved that the optimal coefficients of the staggered one-step forward transversal predictor, H^f, is the solution of the staggered Yule-Walker equation

$$M_z^f H^f = R_z^f \quad (6)$$

Therefore, the staggered forward and backward transversal predictors are optimal in the minimum MSE sense. In practice, the input sequence always contains additive noise, so, M_z^b and M_z^f are non-singular matrixes and the solutions of (5) and (6) always exist.

Based on the above staggered backward and forward transversal predictors, we proposed a staggered lattice predictor structure of order M, as shown in Figure 3. Its signal streams are the same as those of a uniformed lattice predictor but its major elements are time-variant. The input sequence $z(t_n)$, $n \in \{0, 1, \cdots\}$ is of stagger periods and $R_m^b(t_n)$ and $R_m^f(t_n)$ are the reflection coefficients of the mth (1 to M)

stage, $T_m(t_n)$ is delay time of the mth stage, and $e^b_m(t_n)$ and $e^f_m(t_n)$ are the backward and forward prediction errors of the mth stage, at time t_n, b and f the superscripts of backward or forward prediction, respectively. Each stage operation is modularized and the mth stage prediction errors at time t_n are computed as

$$e^f_m(t_n)=e^f_{m-1}(t_n)+R^f_m(t_n)e^b_{m-1}(t_{n-1}),\ m\in\{1,\ 2,\cdots,\ n\},\ n\in\{1,\ 2,\ \cdots,\ M\}, \tag{7}$$

$$e^b_m(t_n)=e^b_{m-1}(t_{n-1})+R^b_m(t_n)e^f_{m-1}(t_n),\ m\in\{1,\ 2,\cdots,\ n\},\ n\in\{1,\ 2,\ \cdots,\ M\}, \tag{8}$$

$$e^f_0(t_n)=e^b_0(t_n)=z(t_n),\ n\in\{0,\ 1,\ \ldots,\ M\} \tag{9}$$

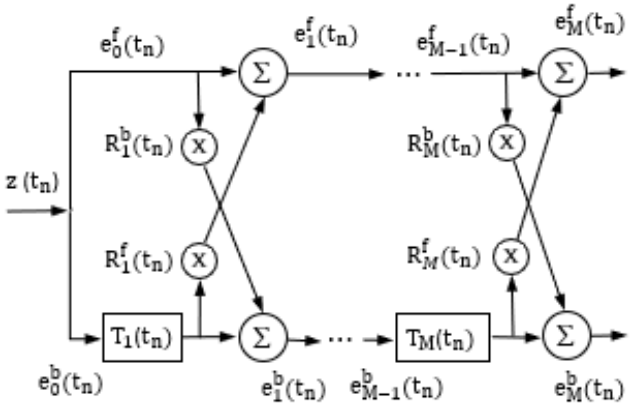

Figure 3. *A stagger-period lattice prediction filter of order M.*

In order to achieve optimal prediction, $R^f_m(t_n)$ and $R^b_m(t_n)$ of each stage are determined by not only the last errors but also observation time t_n, thus, the reflection coefficients of the staggered predictor are time-variant, and with $\{z(t_n)\}$ coming from t_{n-m} to t_n, an order m lattice has $\sum$m forward and backward reflection coefficients, $\sum$m sum of the sequence 1, 2, ⋯, m. In other words, a staggered lattice predictor of order M is composed of all the orders 1 to M lattices at different time. From formulas (7) to (9), given the forward and backward prediction errors at stage m–1, the two-type prediction errors at stage m are calculated in the computationally efficient manner.

Assuming that the input $\{z(t_n)\}$ is stationary, in terms of (7) to (9), the reflection coefficients of mth stage of the staggered lattice predictor are derived in the minimum MSE sense as

$$R^f_m(t_n)=\frac{-E\{e^{\ f}_{m-1}(t_n)\ e^{\ b*}_{m-1}(t_{n-1})\}}{E\{|e^{\ b}_{m-1}(t_{n-1})|^2\}},\ m\in\{1,\ 2,\ \cdots,\ n\},\ n\in\{1,\ 2,\cdots,\ M\}, \tag{10}$$

$$R^b_m(t_n)=\frac{-E\{e^{\ f*}_{m-1}(t_n)\ e^{\ b}_{m-1}(t_{n-1})\}}{E\{|e^{\ f}_{m-1}(t_n)|^2\}},\ m\in\{1,\ 2,\ \cdots,\ n\},\ n\in\{1,\ 2,\cdots,\ M\}, \tag{11}$$

by differentiating $|e^f_m(t_n)|^2$ and $|e^b_m(t_n)|^2$ with respect to $R^f_m(t_n)$ and $R^b_m(t_n)$, respectively, and setting the derivatives to zero. Note that these operations need to apply the Wirtinger calculus [1]. Thus, the two formulas feature the local optimality of the staggered lattice predictor, called the staggered Forward and Backward Error Minimum algorithm. In the case of stationary sequence, one of the staggered predictor's properties is no guarantee that

$$R^f_m(t_n)=R^{b*}_m(t_n),\ m\in\{2,\ 3,\ \cdots,\ n\},\ n\in\{2,\ 3,\ \cdots,\ M\}, \tag{12}$$

except that $R^f_1(t_n)=R^{b*}_1(t_n)$. Another property of the predictor is that its reflection coefficients do not ensure to meet both

$$|R^f_m(t_n)|<1\ \text{ and }\ |R^b_m(t_n)|<1, \tag{13}$$

unlike the uniformed lattice. This is not critical because this structure in Figure 3 is equivalent to an all-zero FIR filter, rather than an all-pole filter of infinite impulse response form. However, the denominators of (10) and (11) are the error powers which may be close to zero, so, the predictor has a instability risk in application. Our many computer tests below verify the issue and give an efficient solution.

Table 2 lists the prediction error powers of five order 4 staggered lattice predictors with five different stagger periods. Two tested stagger-period sequences are still models C-MS0 and C-MS4 in Table 1. The prediction error powers with C-MS0 are from −49.1 to −51.3 dB and with C-MS4 from −38.3 to −35.4 dB, depending on the period scale; these powers have about ±1 dB deviation from those powers of the uniformed predictor in Table 1. These staggered lattice predictors ensure the matches between their reflection coefficients and the input sequence's stagger periods, so they still gain the minimum MSE.

Table 2. *Error powers of stagger-period lattice predictors with stagger-period sequences.*

Periods of Sequences (ms) T1:T2:T3:T4:T5	Sequence models	
	C-MS0	C-MS4
	(dB)	(dB)
2.42:2.92:2.62:2.82:3.12	−51.3	−38.3
2.92:2.62:2.82:3.12:2.42	−49.7	−35.9
2.62:2.82:3.12:2.42:2.92	−50.5	−37.1
2.82:3.12:2.42:2.92:2.62	−50.4	−35.8
3.12:2.42:2.92:2.62:2.82	−49.1	−35.4

3. Global Optimality of the Stagger-Period Lattice Predictor

3.1. Global Optimality of the Staggered Lattice Predictor

Given that a stagger-period sequence is $z(t_n)$, $n\in\{0,\ 1,\ \cdots\}$ and the coefficients of order m (1 to M) forward transversal prediction filter are $h^f_m(t_n,\ \tau^f_j)$, $j\in\{1,\ 2,\ \cdots,\ n\}$, $n\in\{1,\ 2,\ \cdots,\ m\}$, at time t_n, it predicts $z(t_n)$ as shown in Figure 4, when $\{z(t_n)\}$ is coming from t_{n-m} to t_n, number of the forward prediction filters at the different time is $\sum$m. Similarly, given

that the coefficients of order m backward transversal prediction filter are $\{h_m^{b*}(t_n, \tau_j^b)\}$, when it predicts $z(t_{n-m})$ as shown in Figure 5, number of the backward predictors at the different time is $\sum m$ too. Under the condition that forward and backward errors of the orders 1 to m transversal predictors equal those errors of the orders 1 to m lattice predictors in Figure 3, respectively, the reflection coefficients of the $\sum m$ lattice predictors are determined by the coefficients of the $\sum m$ forward and backward transversal predictors as follows,

$$R_m^f(t_n) = h_m^f(t_n, \tau_m^f),\ m \in \{1, 2, \cdots, n\},\ n \in \{1, 2, \cdots, M\}, \quad (14)$$

$$R_m^b(t_n) = h_m^{b*}(t_n, \tau_m^b),\ m \in \{1, 2, \cdots, n\},\ n \in \{1, 2, \cdots, M\} \quad (15)$$

Relations (14) and (15) will be proved in Appendix in the end. The relations indicate that in the case of stagger-period sequences, when the $\sum M$ optimal forward and backward transversal predictors in the minimum MSE sense are given, the $\sum M$ equivalent optimal lattice predictors are uniquely determined.

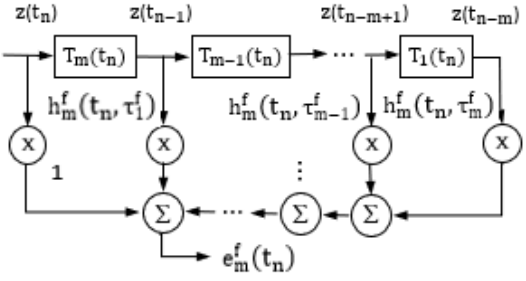

Figure 4. *A forward transversal prediction filter of order m.*

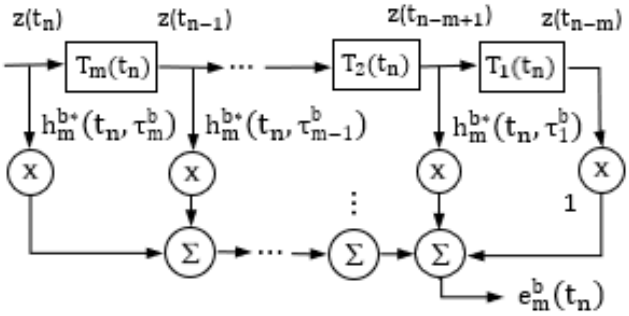

Figure 5. *A backward transversal prediction filter of order m.*

For an example of relations (14) and (15), given a staggered input sequence $z(t_0)$, $z(t_1)$, and $z(t_2)$, the order 2 staggered forward and backward transversal predictors are composed of separate two order 1 and one order 2 coefficient sets at the different time, which determine six equivalent reflection coefficients at the corresponding time as follows.

At time t_1, for the inputs $z(t_0)$ and $z(t_1)$, the order 1 forward and backward transversal coefficients determine the order 1 lattice coefficients,

$$R_1^f(t_1) = h_1^f(t_1, \tau_1^f),\ R_1^b(t_1) = h_1^{b*}(t_1, \tau_1^b)$$

At time t_2, for the inputs $z(t_0)$, $z(t_1)$ and $z(t_2)$, the order 1 and order 2 forward and backward transversal coefficients determine the order 1 and order 2 lattice coefficients, respectively,

$$R_1^f(t_2) = h_1^f(t_2, \tau_1^f),\ R_1^b(t_2) = h_1^{b*}(t_2, \tau_1^b) \text{ and } R_2^f(t_2) = h_2^f(t_2, \tau_2^f),\ R_2^b(t_2) = h_2^{b*}(t_2, \tau_2^b)$$

Note that the other eight transversal coefficients do nothing and are excluded above. Here they are

$$h_1^f(t_1, \tau_0^f),\ h_1^{b*}(t_1, \tau_0^b), \text{ and } h_1^f(t_2, \tau_0^f),\ h_1^{b*}(t_2, \tau_0^b), \text{ and } h_2^f(t_2, \tau_1^f),\ h_2^{b*}(t_2, \tau_1^b),\ h_2^f(t_2, \tau_0^f),\ h_2^{b*}(t_2, \tau_0^b).$$

On the contrary, given that an input sequence is $\{z(t_n)\}$, at time t_n, forward and backward reflection coefficients of order m (1 to M) lattice predictor are $\{R_m^f(t_n)\}$ and $\{R_m^b(t_n)\}$, respectively, as in Figure 3, and forward and backward transversal predictors of order m are $\{h_m^f(t_n, \tau_j^f)\}$, and $\{h_m^{b*}(t_n, \tau_j^b)\}$, respectively, as in Figures 4 and 5, when $z(t_n)$ is coming from t_{n-m} to t_n, under the condition that the prediction errors of the order m forward and backward lattices equal those errors of the order m forward and backward transversal predictors, respectively, the equivalent coefficients of the $\sum m$ staggered forward and backward transversal predictors are determined by the coefficients of the $\sum m$ staggered lattice predictors from low order to high order as follows.

$$h_m^f(t_n, \tau_m^f) = R_m^f(t_n),\ m \in \{1, 2, \cdots, n\},\ n \in \{1, 2, \cdots, M\}, \quad (16)$$

$$h_m^{b*}(t_n, \tau_m^b) = R_m^b(t_n),\ m \in \{1, 2, \cdots, n\},\ n \in \{1, 2, \cdots, M\}, \quad (17)$$

$$h_m^f(t_n, \tau_k^f) = h_{m-1}^f(t_n, \tau_k^f) + R_m^f(t_n)\, h_{m-1}^{b*}(t_{n-1}, \tau_{m-k}^b),\ k \in \{1, 2, \cdots, m-1\},\ m \in \{2, 3, \cdots, n\},\ n \in \{2, 3, \cdots, M\}, \quad (18)$$

$$h_m^{b*}(t_n, \tau_k^b) = h_{m-1}^{b*}(t_{n-1}, \tau_k^b) + R_m^b(t_n)\, h_{m-1}^f(t_n, \tau_{m-k}^f),\ k \in \{1, 2, \cdots, m-1\},\ m \in \{2, 3, \cdots, n\},\ n \in \{2, 3, \cdots, M\} \quad (19)$$

These relations will be proved in Appendix in the end. We call the relations (14), (15), and (16) to (19) the staggered L-D relations. These recursion relations indicate that in the case of a staggered sequences, when an optimal lattice predictor operates in terms of (7) to (9), the equivalent optimal transversal predictors are recursively determined, from low order to high order. Due to the time-varying periods, the optimal transversal predictors of order M have $\sum M$ forward and backward transversal sub-predictors at the different time. At the time t_M, the forward and backward coefficients of the order M transversal predictors can achieve the global optimality from low order to high order in the minimum MSE sense; according to the staggered L-D relations, the corresponding order M lattice predictor at t_M is equivalent to the global optimal transversal predictor. Thus, the full local optimality of a staggered lattice predictor results

in its global optimality.

For an example of relations (16) to (19), given a staggered input sequence $z(t_0)$, $z(t_1)$, $z(t_2)$, an order 2 staggered lattice is composed of six ($2\sum 2$) reflection coefficients. At time t_1, the order 1 lattice coefficients with $z(t_0)$ and $z(t_1)$ determine the order 1 forward and backward transversal coefficients,

$$h_1^f(t_1,\tau_1^f) = R_1^f(t_1),\ h_1^{b*}(t_1,\tau_1^b) = R_1^b(t_1)$$

and at time t_2, the other order 1 lattice coefficients with $z(t_1)$ and $z(t_2)$ determine the other order 1 forward and backward transversal coefficients,

$$h_1^f(t_2,\tau_1^f) = R_1^f(t_2),\ h_1^{b*}(t_2,\tau_1^b) = R_1^b(t_2)$$

and the order 2 lattice coefficients with $z(t_0)$, $z(t_1)$ and $z(t_2)$ recursively determine the order 2 forward and backward transversal coefficients,

$$h_2^f(t_2,\tau_2^f) = R_2^f(t_2),\ h_2^f(t_2,\tau_1^f) = h_1^f(t_2,\tau_1^f) + R_2^f(t_2)\, h_1^{b*}(t_1,\tau_1^b), \text{ and}$$

$$h_2^{b*}(t_2,\tau_2^b) = R_2^b(t_2),\ h_2^{b*}(t_2,\tau_1^b) = h_1^{b*}(t_1,\tau_1^b) + R_2^b(t_2)\, h_1^f(t_2,\tau_1^f)$$

Additionally, the other six transversal coefficients $h_m^f(t_n,\tau_0^f)$ =1 and $h_m^{b*}(t_n,\tau_0^b)$ =1, $m \in \{1, n\}$, $n \in \{1, 2\}$ are known as defined above. Thus, the staggered L-D relations result in computationally efficient transforms, from lattice structure to transversal structure and in reverse.

3.2. Frequency Responses of a Staggered Lattice Filter

Given that input sequence $\{z(t_n)\}$, $n \in (0, 1, \ldots)$, is of N_t-circular stagger periods T_i, $i \in \{1, 2, \cdots, N_t\}$, its average sampling frequency $F_a = N_t / \sum_{i=1}^{N_t} T_i$. When the stagger-period scale meets $T_1{:}T_2{:}\cdots T_{N_t} = k_1{:}\, k_2{:}\cdots k_{N_t}$, the ordered integers $\{k_i\}$ are called the period code of $\{T_i\}$. If $\{k_i\}$ are mutually prime and meet

$$\tau = T_1/k_1 = T_2/k_2 = \cdots T_{N_t}/k_{N_t}, \tag{20}$$

we call the ratio τ the highest common divisor of these periods. Given a staggered backward transversal filter $h_T^b(t_n)$, $n \in \{0, 1, \cdots\}$, its frequency response is defined as [13]

$$H_T^b(f) = \sum_{n=0}^{\infty} h_T^b(t_n) e^{-j2\pi f t_n},\ f \in [-F_p/2,\ F_p/2], \tag{21}$$

where $F_p = 1/\tau$ is called frequency response cycle of the staggered filter, it is also spectrum cycle of the sequence $\{e^{-j2\pi f t_n}\}$ and equal to $F_a \sum_{i=1}^{N_t} k_i/N_t$. In practice, $\{h_T^b(t_n)\}$ is always windowed to a length, e.g., N_p, the frequency response in (21) is time-variant and is redefined as

$$H_T^b(f, t_n) = \sum_{n=0}^{N_p-1} h_T^b(t_n) e^{-j2\pi f t_n} \tag{22}$$

When the superscripts b are substituted with f and the periods of $\{t_n\}$ are inverse, (22) represents the forward transversal filter response $H_T^f(f, t_n)$. Similarly, the frequency response of a staggered lattice filter of limited order is time-variant too. For an order M staggered lattice filter, the frequency response of its backward prediction is defined as

$$H_L^b(f, t_n) = e_M^b(t_n, e^{-j2\pi f t_n}),\ f \in [-F_p/2,\ F_p/2], \tag{23}$$

where $e_M^b(t_n, e^{-j2\pi f t_n})$ is the backward prediction output at time t_n when the input is $\{e^{j2\pi f t_n}\}$. When the superscripts b in (23) are substituted with f, it represents the forward prediction frequency response of the lattice filter, $H_L^f(f, t_n)$. Both the frequency responses are related to the reflection coefficients $\{R_m^f(t_n)\}$, $\{R_m^b(t_n)\}$, periods $\{T_i\}$, and the stagger-period scale, so, they are different; in contrast, for a uniformed lattice filter, its forward and backward responses are the same. Figure 6 shows four frequency responses of the forward and backward transversal filters and equivalent lattice filter of order 4. The two transversal filters are the solutions of (5) and (6) and the lattice filter is obtained by L-D relations (14) and (15). The covariance matrix is calculated with a clutter sequence of double-Gaussian spectrum, which mixes the clutter C-MS0 with another clutter, P_w 30 dB, F_w 72 Hz and D_w 14.4 Hz [1]. The stagger-period scale is 2.42:2.92:2.62:2.82:3.12 ms; its average pulse repeat frequency (PRF) is 360 Hz. The green and red curves represent the forward and backward lattice predictor responses, respectively; the black and dark red represent the forward and backward transversal predictor responses, respectively. We observe that the two forward responses are the same and overlapped, and the two backward responses are so too. However, the forward and backward responses are not exactly the same due to inverse order of periods. The resulting responses would be the same, if the test sequence was uniform-period. The four responses in Figure 6 have a deep notch of about −55 dB at 0 Hz and a wide notch of about −18 dB between 10 and 90 Hz. Such frequency response shapes match the test clutter spectrum and the entire overlaps of the forward/backward responses verify the staggered L-D relations (14) and (15).

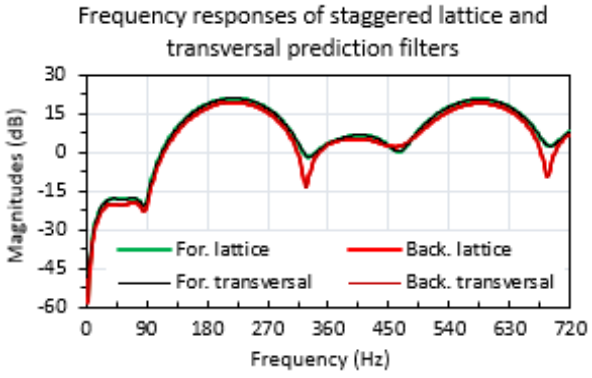

Figure 6. *Frequency responses of a staggered lattice and its equivalent transversal prediction filters.*

[1] In this paper, all clutter spectra are Gaussian. P_g, D_g, and F_g denote power normalized to noise, standard deviation bandwidth, and center frequency of mountain or terrain clutter, respectively; P_w, D_w, and F_w the corresponding parameters of weather clutter; P_t and F_t the corresponding parameters of Doppler target signal.

4. Convergence Performance of a Staggered Lattice Predictor

4.1. Algorithms of Staggered Reflection Coefficients

In the case of uniform-period sequence, basic algorithms of lattice reflection coefficients include the Forward and Backward Error Minimum, Geometric Mean and Harmonic Mean [14, 15]. For the stagger-period stationary sequence, given a staggered lattice predictor of order M as shown in Figure 3, here we present three similar algorithms. The staggered Forward and Backward Error Minimum is just (10) and (11) in section 2, the two formulas are individually optimal to forward or backward prediction in the minimum MSE sense. The staggered Geometric Mean algorithm is

$$R_m^f(t_n)=R_m^{b*}(t_n)=\frac{-E\{e_{m-1}^f(t_n)\, e_{m-1}^{b*}(t_{n-1})\}}{[E\{|e_{m-1}^b(t_{n-1})|^2\}\,E\{|e_{m-1}^f(t_n)|^2\}]^{1/2}},\ m\in\{1,\ 2,\ \cdots,\ n\},\ n\in\{1,\ 2,\ \cdots,\ M\} \tag{24}$$

Obviously, the algorithm makes the forward and backward coefficients equal in magnitude, and its operation is relatively simple; however, its optimality does not exactly hold, so, this algorithm is not suitable for the stagger-period sequence. The staggered Arithmetic Mean algorithm is

$$R_m^f(t_n)=\frac{-E\{e_{m-1}^f(t_n)\, e_{m-1}^{b*}(t_{n-1})\}}{(1-\alpha)E\{|e_{m-1}^f(t_n)|^2\}+\alpha E\{|e_{m-1}^b(t_{n-1})|^2\}},\ m\in\{1,\ 2,\ \cdots,\ n\},\ n\in\{1,\ 2,\ \cdots,\ M\}, \tag{25}$$

$$R_m^b(t_n)=\frac{-E\{e_{m-1}^{f*}(t_n)\, e_{m-1}^{b}(t_{n-1})\}}{\alpha E\{|e_{m-1}^f(t_n)|^2\}+(1-\alpha)E\{|e_{m-1}^b(t_{n-1})|^2\}},\quad m\in\{1,\ 2,\ \cdots,\ n\},\ n\in\{1,\ 2,\ \cdots,\ M\}. \tag{26}$$

where α is balance factor and its value is taken within 0.5 to 1. For the Arithmetic Mean algorithm, the denominators put different weights on the forward and backward error powers, and two unequal reflection coefficients are given. When α=1, (25) and (26) turn into the staggered Forward and Backward Error Minimum algorithm; when α=0.5, (25) and (26) into the staggered Harmonic Mean algorithm. Thus, the Arithmetic Mean algorithm is relatively flexible and maintains optimality. For a stagger-period lattice, its forward prediction periods are inversion of its backward prediction periods, generally, $E\{|e_{m-1}^f(t_n)|^2\}$ and $E\{|e_{m-1}^b(t_{n-1})|^2\}$ are unequal, so are $R_m^f(t_n)$ and $R_m^b(t_n)$. Only the Forward and Backward Error Minimum algorithm is exactly optimal to individual forward or backward prediction. Similarly to the Burg algorithm's proof [1], the staggered Arithmetic Mean algorithm with α=0.5 guarantees the minimum sum of forward and backward MSEs.

All the reflection coefficient algorithms above are to involve the ensemble mean processing. In a practical application, they are unfeasible due to limited time series. We have to seek an applicable method to estimate the reflection coefficients, whose convergence is fast and stable in a specific application. The staggered Arithmetic Mean algorithm behaves with optimality and flexibility relative to the other algorithms, so, we focus on it for applicable coefficient estimation. Assuming that an input sequence is stationary and ergodic, denoted by $z(t_n)$, $n\in\{0,\ 1,\ \cdots\}$, we may use least square error (LSE) time averages to substitute for the ensemble mean operation. Based on the Arithmetic Mean algorithm, we present a method to estimate the reflection coefficients of the staggered lattice predictor, called the staggered Arithmetic Mean method, as

$$\hat{R}_m^f(t_n)=\frac{-\sum_{l=1}^{L_w} e_{m-1}^f(t_n;\,l)\, e_{m-1}^{b*}(t_{n-1};\,l)}{\sum_{l=1}^{L_w}[(1-\alpha)|e_{m-1}^f(t_n;\,l)|^2+\alpha|e_{m-1}^b(t_{n-1};\,l)|^2]},\ m\in\{1,\ 2,\ \cdots,\ n\},\ n\in\{1,\ 2,\ \cdots,\ M\}, \tag{27}$$

$$\hat{R}_m^b(t_n)=\frac{-\sum_{l=1}^{L_w} e_{m-1}^{f*}(t_n;\,l)\, e_{m-1}^{b}(t_{n-1};\,l)}{\sum_{l=1}^{L_w}[\alpha|e_{m-1}^f(t_n;\,l)|^2+(1-\alpha)|e_{m-1}^b(t_{n-1};\,l)|^2]},\ m\in\{1,\ 2,\ \cdots,\ n\},\ n\in\{1,\ 2,\ \cdots,\ M\}, \tag{28}$$

where M is order of the staggered lattice predictor, α is the balance factor, L_w is the length of averaging window, and l is the batch number. (data $z(t_n)$, $n\in\{0,\ 1,\ \cdots,\ M\}$ is a batch; L_w batches form a window.) Equations (27) and (28) are a type of LSE estimation of the reflection coefficients in the LSE sense. The M+1 data of $\{z(t_n{:}l)\}$ along t_n are correlated while the L_w batches of $\{z(t_n{:}l)\}$ along l are required to be independent and have the same statistics; so, selection of the input sequence blocks $\{z(t_n;l)\}$ is crucial. If the averaging batches are not independent, the estimation efficiency is very low [16]. When α=1, (27) and (28) turn into the staggered Forward and Backward Error Minimum method; when α=0.5, (27) and (28) into the staggered Harmonic Mean method.

4.2. Convergence Performance of a Staggered Lattice

In the case of a stagger-period stationary sequence, convergence performance of a lattice predictor is its behavior of estimation approaching to the optimum goal, e.g., the reflection coefficient, prediction error, etc., called the observation goal. This can be evaluated from three aspects: the estimated results' deviation, expended time, and stability. Some references presented their researches on convergence performances of uniform-period lattices, they adopted analytic derivations or computer simulations [16, 17]. When the deriving result or simulating estimate reaches an assigned value, number of the used samples or the expended time is referred to as the convergence rate of the estimation method.

Generally, the computer simulation is more practicable. The smaller the number of the run off samples is, the faster the convergence rate of the method is.

4.2.1. Reflection Coefficients as the Goal

Consider at first that the observation goal is the reflection coefficients. For a stationary sequence, the Arithmetic Mean method computes the prediction errors with multi-batch data and averages them on a window length L_w, then computes $\widehat{R}_m^f(t_n)$ and $\widehat{R}_m^b(t_n)$ in terms of (27) and (28). Usually, the estimates approximate to the ensemble means $R_m^f(t_n)$ and $R_m^b(t_n)$ with L_w increase. To examine the convergence performance, we conducted computer simulation rather than a analytic derivation. Referring to radar environmental clutters [9, 12], we generated the stagger-period complex sequences featuring mountain and weather returns, whose spectra are the double-Gaussian: mountain P_g 60 dB, F_g 0 Hz, D_g 3.6 Hz, and weather P_w 30 dB, F_w 72 Hz, D_w 14.4 Hz. The stagger-period parameters are the same as assigned in Figure 6. The order 4 staggered lattice predictor has 20 complex reflection coefficients totally. If we present convergence curves of all the reflection coefficients, they will occupy a lot space in this paper. Therefore, we select the reflection coefficient estimates of the last stage as the observation goal. The convergence behavior of the Arithmetic Mean method with α=0.8 is shown in Figure 7. The four thin curves represent estimated (E) complex coefficients $\widehat{R}_4^f(t_4)$, $\widehat{R}_4^b(t_4)$, respectively and the four thick straight lines represent optimal (O) (minimum MSE) complex coefficients $R_4^f(t_4)$, $R_4^b(t_4)$, respectively. The optimal coefficients result from solutions of (5) and (6) for the transversal coefficients and the L-D relations (14) and (15) for the lattice coefficients. The four colors, black, green, red, and blue, denote real, imaginary (Imag) of the forward (F) coefficients, and real, Imag of the backward (B) coefficients, respectively. For example, the curve real E F denotes real of the estimated forward coefficient; the curve real O F denotes real of the optimal forward coefficient. We observe that these reflection coefficient estimates tend towards stability after length of the averaging window L_w is larger than 20, but the deviations from the optimal coefficients are still large, e.g., Imag E F is 0.276 at L_w=74, far away from the optimal 0.553. In the initial estimation L_w<10, these curves may swing strongly, e.g., the real E F max reaches 1.086 (unseen) at L_w 2 but the real O F is −0.601. Thus, the test curves deviate from the optimal curves much and the convergence behavior shows instability.

We take another try with larger α. All the test conditions are the same as those assigned in Figure 7 except α=0.99. Figure 8 shows the tested convergence behavior. We observe that deviations from the optimal coefficients are much less than those in Figure 7 after L_w is larger than 10. For example, Imag E F max is 0.723 at L_w 37, not big deviation from the optimal 0.553; real E F max is −0.765 at L_w16, not big deviation from the optimal −0.601 either. In initial estimation, the convergence still behaves with very big swings from 1.83 (unseen) to −0.99. This indicates that the larger the α is, the less the estimate variance is but the worse the initial estimation stability is.

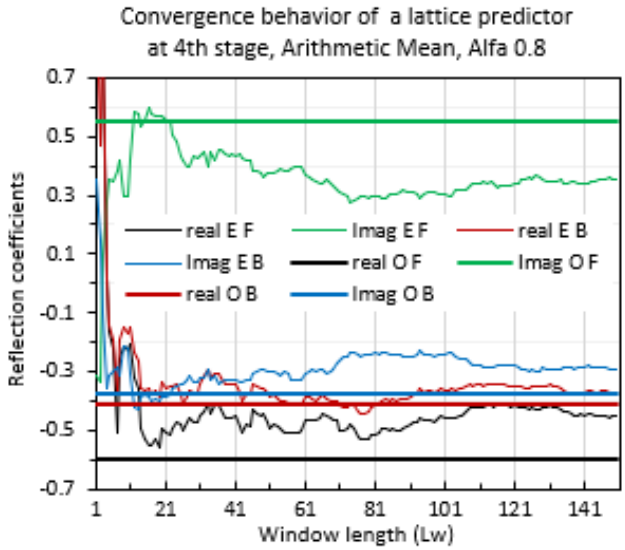

Figure 7. *Convergence behavior of reflection coefficients of an order 4 staggered lattice predictor with α=0.8.*

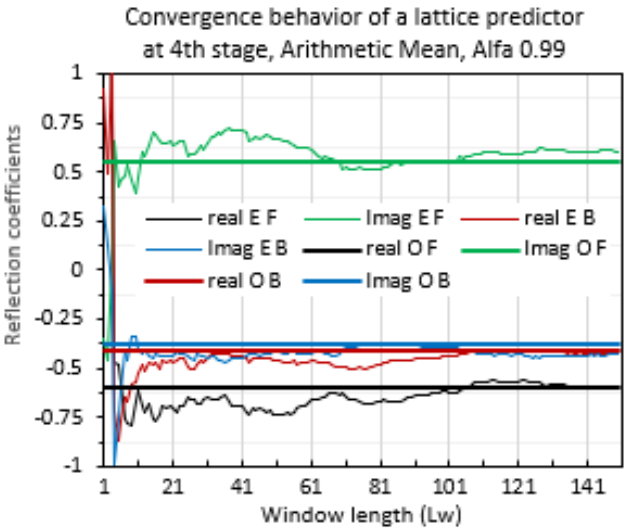

Figure 8. *Convergence behavior of reflection coefficients of an order 4 staggered lattice predictor with α=0.99.*

In summary, the two-test results verify that 1) the Arithmetic Mean method is effective to estimate the staggered reflection coefficients; 2) when α is large, the convergence behaves with fast rate and small deviation from the optimal coefficients; 3) no matter α is small or large, the convergence behaves with the strong swings of reflection coefficients in the initial estimation; the swings result from the small-sample prediction error estimates in the denominators of (27) and (28), the problem can be efficiently solved by increasing the window length L_w, e.g., larger than 10.

4.2.2. Prediction Errors as the Goal

The above observation goal focuses on two reflection coefficients of the last stage and these results do not represent convergence behaviors of the coefficients of the other stages. It is a huge work to evaluate the 20 reflection coefficient convergences. Alternatively, we select prediction errors of the last stage as the observation goal; the two prediction errors

represent the contributions of all the stages, so, give a global examination. The forward and backward error power estimates of the last stage of an order M lattice predictor are, respectively,

$$P_a^f=\sum_{l=1}^{L_w}|e_M^f(t_M:l)|^2/P_z, \quad (29)$$

$$P_a^b=\sum_{l=1}^{L_w}|e_M^b(t_M:l)|^2/P_z, \quad (30)$$

where P_z is average power of the input sequence $\{z(t_n:l)\}$ on L_w batches. $e_M^f(t_M:l)$ and $e_M^b(t_M:l)$ are computed in terms of (7) to (9), with the estimated reflection coefficients in section 4.2.1. Under the same test conditions as those assigned in Figure 7, Figure 9 shows the convergence behavior of the forward and backward error powers of the lattice predictor with α 0.8. The thick straight lines represent the optimal prediction error powers and thin curves represent the estimated error powers; the red and black denote backward and forward prediction, respectively. We observe that the two estimated curves behave with very deep notches in initial estimation, unseen depth max −84.9 dB. After entering stable state with L_w increase, e.g., >21, the two thin curves are about 2 dB higher than the thick lines individually. Note that although the initial prediction errors are lower than the minimum MSE, there exists a big risk of instability.

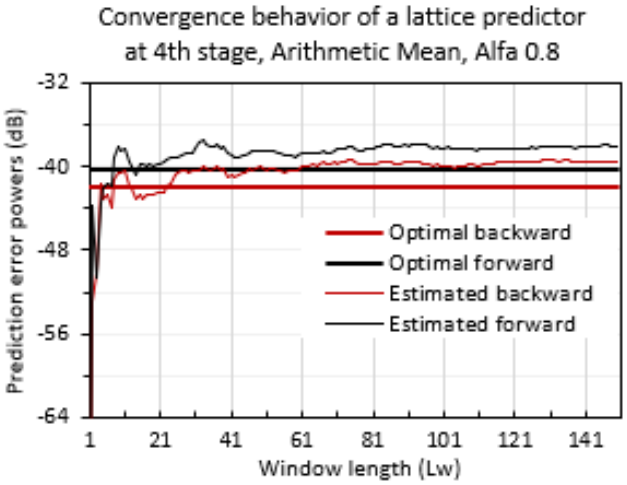

Figure 9. *Convergence behaviors of prediction errors of an order 4 lattice predictor with α 0.8.*

In order to improve the convergence performance, we take another try on different α and still select the prediction error as the goal. Under the same test conditions as those assigned in Figure 9 except α=0.99, Figure 10 shows the convergence behavior of the lattice predictor. The thick straight lines represent the optimal prediction errors and the thin curves represent the estimated errors; the red and black represent backward and forward prediction, respectively. We observe that the two estimated error powers behave with deeper notches in initial estimation, the unseen notch max −198 dB; two thin curves asymptotically enter the stable state when L_w >10 and approach close to the optimal error lines individually when L_w>70. So, this convergence performance is better than that with α 0.8.

In summary, these test results verify that 1) the Arithmetic Mean method is effective to work with the staggered lattice predictor; 2) the error estimates always enters the stable state with L_w increase and even approach close to the optimal values with enough large L_w; 3) in the initial estimation, the prediction error curves always behave with very deep notches when α ≥0.8, so, there exists a big risk of instability. The notches are caused by the small-sample error powers in the denominators of (27) and (28), it can be efficiently solved with large-sample average, e.g., L_w>10.

No matter the observation goal is the reflection coefficients or prediction errors, the convergence performances of the staggered lattice predictor are acceptable, depending on the balance factor, window length, and order of the lattice predictor. In practice, for a specific application, one needs to conduct the computer simulation to accurately know the best values of the parameters. When simulating, independence of the averaging batches can not be inconsiderable and bad independence will result in low convergence rate or large predictor order.

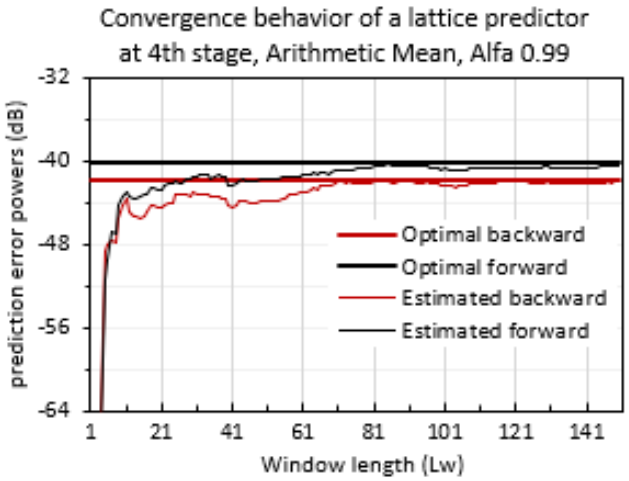

Figure 10. *Convergence behaviors of prediction errors of an order 4 lattice predictor with α 0.99.*

5. Learning Characteristic of a Staggered Lattice Predictor

Learning characteristic of a lattice predictor is its ability to track statistics of a nonstationary sequence. In a stationary sequence, the more the averaging batches to estimate $R_m^f(t_n)$ and $R_m^b(t_n)$ are, the smaller the coefficient estimate variances are. Obviously, in a nonstationary sequence, this rule does not hold due to varying statistics of the segmental batches. When an aircraft signal intrudes into a stationary clutter, the disturbed clutter turns into a nonstationary clutter. In study of this topic, we prefer to use prediction errors as the observation goal to take more exact evaluation. Later, we also add frequency responses of a lattice predictor as the third observation goal.

5.1. Learning Characteristic in Nonstationary Clutter

In the case of a nonstationary clutter, due to the varying statistics, it is inaccurate to evaluate learning characteristic with the same method in section 4. Specifically, the average prediction errors over large samples in range bins can not efficiently reduce the variance. We select the same staggered lattice predictor as that in section 4. Considering a clutter with quasi- or short-term stationarity, its reflection coefficients are still estimated in terms of (27) and (28), with small L_w, despite the ergodicity; then prediction error estimates from the lattice outputs are averaged over the L_w independent batches. The assigned nonstationary clutter is returns from a mountain (stationary) and weather (nonstationary) around it, of double-Gaussian spectra: P_g 60 dB, F_g 0 Hz, D_g 3.6 Hz, and P_w from 10 to 40 dB along range bins 1 to 150, F_w 72 Hz, D_w 14.4 Hz. The stagger-period parameters are the same as assigned in Figure 6. The best window length depends on the extent of the clutter non-stationarity [18] and L_w is selected as 5, 10, and 15 for comparing. Figure 11 shows the prediction error powers of the staggered lattice predictor with Arithmetic Mean method, α 0.99 and L_w10. The thick and thin curves represent the optimal and estimated error powers, respectively; the black and red denote the forward and backward predictions, respectively. We observe that the two thick curves are stably going up along the range bins; the two fluctuant thin curves are following the thick curves, going up, of a few dB positive bias, and the deviations from the optimal curves are within +10/−6 dB. The smaller the L_w is, the smaller the bias is but the bigger the curves' fluctuation is; the learning curves with L_w 5 and 15 are omitted. Thus, the staggered lattice predictor is really learning the input clutter statistics; however, it is impossible to close track the optimal curves as in the stationary clutter. The learning curves show no thing in the first 4 bins and in the last 4 bins, which are called initiation and termination bins, respectively, because Arithmetic Mean method averages the errors over L_w bins and the estimate represents the error in the median bin only, unlike the situation in stationary clutter.

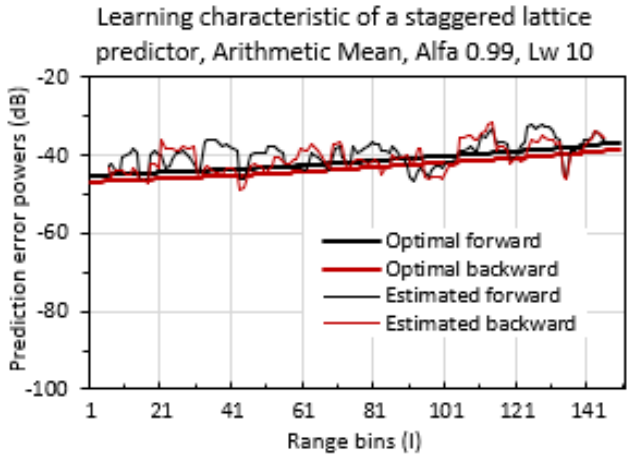

Figure 11. *Learning characteristic of a staggered lattice predictor in nonstationary clutter.*

From Figure 11, we know one side of the learning ability of the staggered lattice predictor, prediction error track. To evaluate another side of the ability, we select frequency response estimate as the observation goal. For comparing effects of the two-type goals, the test conditions are the same as those in Figure 11. We select three pairs of the reflection coefficient estimates, which locate in three range bins, 5, 75 and 145, where the returns have different weather clutter powers, 10.8, 24.9, and 39 dB, respectively. Three frequency responses of the 4th stage of the corresponding lattice predictors, $H_L^f(f,t_4)$, are computed. Figure 12 shows the frequency responses in the three bins, denoted by the black, red, and green, respectively. We observe that the three curves show a deep notch at 0 Hz, about −55 dB, and different depth notches in the frequency range of 20 to 110 Hz, which adapt the different powers of weather clutter. The response in bin 5 has no notch due to a mild weather return; the response in bin 75 has about −15 dB notch relative to the black due medium weather; the response in bin 145 about −30 dB notch due to heavy weather. The frequency responses indicate the great learning ability of the predictor in the stable mountain clutter plus varying weather clutter. Additionally, we also see that the blind speed problem of a Doppler radar is solved well by the stagger-period emission, i.e., the notches with the uniform-period emission disappear at the multiple of pulse repeat frequency, e.g., around 360, 720 Hz.

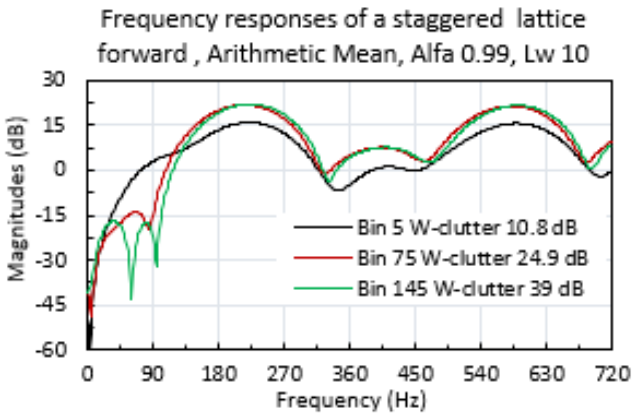

Figure 12. *Frequency responses of a staggered lattice predictor in nonstationary clutter.*

5.2. Learning Characteristic in Clutter Plus Target Signal

We have known from the above section 5.1 that the staggered lattice predictor behaves with great learning ability in the nonstationary clutter. In a radar environment, we also concern with the target signal embedded in a background clutter. Typically, radar returns result from a mountain and weather echoes plus an aircraft echo. It is not clear to evaluate the learning ability by observing the prediction errors in such a situation. Specifically, the radar returns, for example, are composed of mountain P_g 60 dB, F_g 0 Hz, D_g 3.6 Hz, and weather P_w 10 dB, F_w 72 Hz, D_w 14.4 Hz, plus two aircrafts different P_t 5 and 20 dB, the same F_t 432 Hz. The lattice predictor and stagger-period parameters are the same as assigned in Figure 11. Figure 13 shows the resulting frequency responses. The black and green thin curves represent the responses of forward prediction with the

clutter plus aircrafts P_s 5 and 20 dB, respectively, and the red thick curve the response with the clutter only. We observe that the three curves have deep, narrow notches about −60 dB to adapt the strong mountain clutter; the two thin curves do not drops in the frequency range of 20 to 110 Hz for the weather clutter, but they show about 10 dB notch relative to the red curve at 432 Hz for the 5 dB aircraft and about 16 dB notch for the 20 dB aircraft; in contrast, the red thick curve has a shallow drop in the range of 20 to 110 Hz for the weather clutter, but does not form any drop around 432 Hz due to no aircraft. These shapes accurately adapt the features of the input clutters and aircraft signal. Thus, the staggered lattice predictor behaves with great learning ability no matter in the undesired clutters or in the undesired clutter plus desired target signal. On the other hand, this effect alerts us a fact that a single lattice predictor will reject both the clutter and target if we simply apply it in a signal detection field.

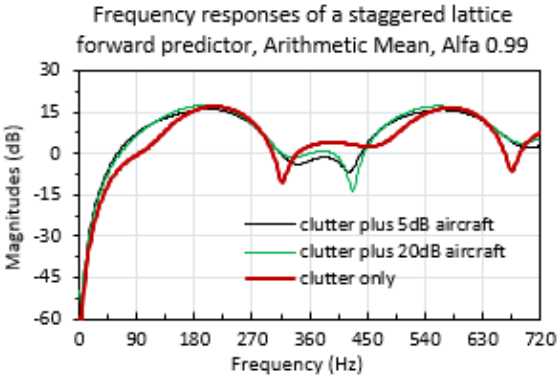

Figure 13. *Frequency responses of a staggered lattice predictor in stationary clutter and clutter plus aircraft.*

6. A Knowledge-Based Block Lattice Predictor for MTI

In order to adaptively detect an aircraft signal submerged in multiple clutters, the lattice prediction filter is a great selection. The stagger-period emission is an efficient technology to solve ambiguity of range and velocity resolutions of a Doppler radar. Pulse-coded compression waveform is an essential emission waveform to detect weak aircraft returns. The staggered lattice predictor presented above is compatible with the two technologies. Two-dimensional radar returns represent an area returns of range echoes (independent) versus azimuth echoes (coherent). The lattice reflection coefficients are estimated with a batch of contiguous, stagger-period azimuth returns; then, the coefficient estimates are averaged over the adjacent range bins to reduce variance. The operation is based on a data block and the resulting lattice predictor is called the staggered block lattice predictor (SBLP). When the SBLP was tested to detect an aircraft signal submerged in the multiple clutters, we found some issues. A typical one is that the reflection coefficient estimates feature both the clutters and aircraft signal as shown in Figure 13. To ensure that the coefficients feature the clutters only, artificial intelligence (AI) activity needs to be incorporated, then, we developed a knowledge-based SBLP. The so-called knowledge means radar professionals' knowledge. The more complete the knowledge is, the more accurate the SBLP's judgment is.

Object echoes of consecutive pulses emitted by an MTI radar, in the same range's bins, are correlated and have a Doppler frequency; generally, an aircraft Doppler frequency is different from a terrain or weather Doppler frequency. The clutter returns exist within a big area of range vs. azimuth and are weakly correlated, of low Doppler frequencies. The aircraft return exists in batches of multi-range vs. multi-azimuth bins and is strongly correlated, of relatively high Doppler frequency. These are basic knowledge of the MTI radar returns. Thus, before estimating the reflection coefficients, the SBLP needs to learn, to analyze and to judge the coming return block to roughly judge its identification. For example, the SBLP can estimate the reflection coefficients only when the current input is judged as a clutter; otherwise, the SBLP throws away the clutter and aircraft both from the filter output. In a nonstationary clutter area, A strong clutter block has a higher lever than a weak clutter block, then, the strong clutter block may be judged as existing an aircraft and a false alarm is caused. Thus, in the realistic application, it is essential to exploit the priori knowledge for the SBLP to intelligently reject background clutters and to extract the intermittent aircraft signal.

After generating the return data of radar environments, we tested the SBLP's behaviors and found some rules. Based on the coming return's region and the output's feature, the SBLP can analyze if an aircraft signal exists in the current block. To raise the target detection rate, the SBLP filters the current data block by the lattice coefficients estimated on the last input data block which is judged there exists no aircraft. To reduce the false alarm rate, the SBLP needs to judges if the current input data block is 1) in a region from non-clutter to clutter or in the reverse region or 2) in a transition region from single model to dual-model clutter or in the reverse region. If so, the SBLP rejects the judged "aircraft". An AI SBLP filter which achieve the above two tasks needs to execute five essential heuristic strategies. The prerequisites for these strategies are: 1) the MTI radar emission with stagger-period repeat pulse and phase-coded pulse compression, 2) two-dimensional returns of azimuth batch vs range bins, 3) clutter backgrounds of a mountain, forested terrain, and changing weather, and 4) the SBLP filter as described in this paper. The five strategies are: 1) Estimating Block and Filtering Block. An coming data block judged to be of clutter only is called the estimating block. Its data are used to estimate the current lattice coefficients; then, the coefficients are used to filter the next data block, which is called the filtering block. 2) Terrace Indication and Target Detection. The lattice filter output always delivers a terrace-like waveform of phase-code length when an aircraft return exists in the coming data, then the segmental output waveform is called the terrace, always higher than the clutter around it. The SBLP utilizes $P_f / P_p \geq 2$ as a preliminary criterion to judge target existence in the filtering block, P_p is

the power mean of estimating block output and P_f is the power mean of filtering block output. When a terrace data length is larger than the compression code length, the filtering block is rejudged to be in a clutter transition region and turns into an estimating block to eliminate the false alarm. 3) Lattice Coefficient Map. When an target detection is done, its reflection coefficients are recorded in a database with the range bin number and azimuth bin number and a reference block is set up; the database recording all the reference blocks is called lattice coefficient map (LCM), and updated if necessary. 4) Space Delay. We use the estimated reflection coefficient of an estimating block or a reference block to filter data of the next adjacent block, the operation is called space delay. It is a key technique of target preservation. 5) Initialization. For the return data in range bins near the surveillance radar site, e.g., within a few km, the data are always non-aircraft returns, so, the initial data block all are the estimating blocks and the reflection coefficient estimates are used to filter in initial short-range search.

In order to examine the SBLP filter for MTI and to verify the five strategies, several clutter models were assigned to represent stationary and nonstationary returns representing realistic radar environments possible [19, 20]. One of our tests is to examine detection performance of the SBLP MTI in a high mountain plus mild weather environment, whose clutter spectra are P_g 60 dB, D_g 3.6 Hz, F_g 0 Hz and P_w 10 dB, D_w 14.4 Hz, F_w 72 Hz individually. Two weak aircrafts are located in range bins 31 and 101, their spectral parameters are P_t 5 and 10 dB, respectively, meaning very low signal-clutter-ratios (SCRs) −55, −50 dB, e.g., stealth, and F_t 175 Hz, meaning low radial speed. The operation parameters of SBLP MTI are: lattice order 4, a batch length Np 5; pulse stagger-period scale 2.415:2.919:2.617:2.818:3.12 ms, and average PRF 360 Hz. The runs of m-sequence phase-code for pulse compression are 2211214111131235. The reflection coefficients are estimated with the Arithmetic Mean method, the balance factor α 0.99, and window length L_w 15. The target detection criterion is $P_f / P_p \geq 2$. The detection performance of the SBLP MTI is shown in Figure 14. The three power curves represent the SBLP input, the SBLP output, and the pulse compressor output, denoted by the blue, black and red, respectively. We observe that the input power curve looks stationary, around 60 dB, and two aircraft signals are completely submerged in the clutters; the SBLP output power curve has two terraces located over bins 31 to 61 and bins 101 to 131, respectively, the former looks rugged due to SCR −55 dB and the latter looks relatively even due to SCR −50 dB. The pulse compression output power curve has two obvious peaks, locating in bins 31 and 101 individually; the latter is about 5 dB higher than the former, indicating that the two aircrafts are detected correctly. Thus, the detection performance of the SBLP MTI is satisfactory and the heuristic strategies are efficient in the strong dual-model stationary clutter plus weak aircraft returns.

The second test is to examine detection performance of the SBLP MTI in a nonstationary double-model clutter arising from forested terrain and changing storm environment. The terrain spectrum is P_g 55 dB, D_g 10.8 Hz, and F_g 0 Hz, meaning a strong stationary return, and the storm spectrum is P_w 10 to 40 dB along range bins 1 to 150, D_w 14.4 Hz, and F_w 72 Hz, meaning an intensity-varying nonstationary return. Two weak targets have the same features as those assigned in Figure 14 test. The other test conditions, such as the stagger-period emission, pulse compression, and SBLP filter, are also the same as those assigned in Figure 14. Figure 15 shows the detection performance of the SBLP MTI in the nonstationary clutter. The three power curves represent input of the MTI, output of the SBLP, and output of the pulse compressor, denoted by the blue, black, and red, respectively. We observe that the input power curve looks nonstationary, about 50 to 53 dB along the full range bins, due to the intensity-increasing storm return; the two aircraft signals are completely submerged in the clutters. The SBLP output curve has two rugged terraces due to the low SCR and clutter instability, located within the bins 31 to 61 and 101 to 131, respectively. The compressor output curve still has two obvious peaks, locating in bins 31 and 101 individually; the latter is about 5 dB higher than the former, indicating that the two aircrafts are correctly detected although the lattice coefficient estimation is more rough in the nonstationary clutter. Thus, the target detection and false alarm control of the SBLP MTI are still great and the heuristic strategies are efficient in the nonstationary clutter.

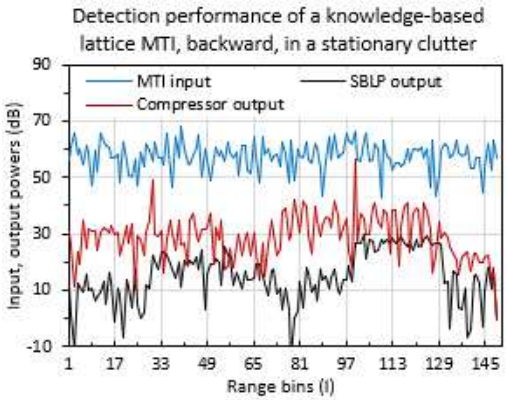

Figure 14. *Detection performance of a knowledge-based SBLP MTI in stationary clutter.*

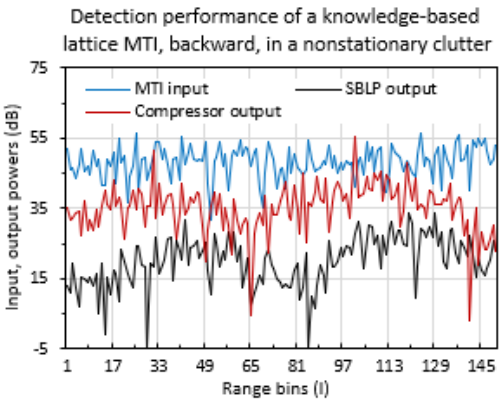

Figure 15. *Detection performance of a knowledge-based SBLP MTI in nonstationary clutter.*

7. Conclusions

In the case of the stagger-period sequence, the staggered lattice predictor is an efficient adaptive processor for predicting or filtering. In the previous five sections, we proposed some new concepts, theories, and algorithms related to the staggered lattice predictor; and conducted many computer simulations to verify validity of the theoretical analyses and mathematic derivations. In order to apply them in an MTI radar, several heuristic strategies are incorporated and the knowledge-based SBLP MTI is illustrated in the stationary and nonstationary clutters plus weak aircraft signals. The research results are summarized as follows.

i). In stagger-period sequence processing, the staggered lattice predictor is an essential topic, especially for adaptive filtering. The staggered lattice predictor has a modularized structure, low sensitivity of coefficient word-length, and less computation load. The staggered lattice predictor has a linear, time-variant property and has ∑M forward and backward reflection coefficients with order M, but the uniformed predictor has M forward and backward reflection coefficients. The complex structure is due to necessary match between the predictor's delay units and the stagger periods of input sequence.

ii). The reflection coefficient algorithm of a staggered lattice predictor, the staggered Forward and Backward Error Minimum, is presented and its local optimality in the minimum MSE sense is proven by means of the Wirtinger calculus. The staggered L-D recursion relations are proposed and proved in the Appendix. They indicate that given the ∑M staggered forward and backward transversal coefficients, the uniquely equivalent ∑M staggered forward and backward reflection coefficients are determined; conversely, given the staggered reflection coefficients, the equivalent transversal coefficients are recursively determined from low order to high order. The complexity also arises from the time-variant property of the two-type predictors. Global optimality of a staggered lattice predictor in the minimum MSE sense is deduced with the staggered L-D relations.

iii). The staggered Arithmetic Mean algorithm is presented and its optimality and flexibility are indicated. When balance factor α =1, this algorithm turns into the staggered Forward and Backward Error Minimum algorithm; when α =0.5, it turns into the staggered Harmonic Mean algorithm. For applying this algorithm to a realistic field, the Arithmetic Mean method is produced so that the staggered reflection coefficients of ensemble mean are substituted with time-average coefficient estimates. Its effectiveness depends on two items: the balance factor α and averaging window length L_w. α is taken between 0.5 and 1, and the larger the α is, the less the variance of the coefficient estimates is, but the higher the instability risk of the initial estimates is. In a stationary sequence, when the L_w is larger than 20, the curves of the reflection coefficient and prediction error estimates get into stable state, even the estimate curves approach close to the optimal values. The staggered lattice predictor behaves with great convergence performance.

iv). In the test with the nonstationary clutter, the staggered lattice predictor has to track the short-term statistics to estimate the prediction errors. The large window length covers wide-range statistics, the resulting learning curve causes a bias and can not exactly represent the statistics in each segment of the full range bins. In addition, the instability risks in the initial estimation are observed, this problem can be solved through increasing the window length. No matter we observe the convergence behavior or learning characteristic, the larger the balance factor is, the faster the convergence rate of the staggered predictor is. Examples of the great learning characteristic are illustrated with L_w=10 and α=0.99. Thus, in considering a specific application, selecting the proper balance factor and averaging window length can achieve the best lattice predictor possible.

v). A knowledge-based lattice MTI with stagger-period emission incorporates radar professionals' knowledge to logically analyze coming data block when it suppresses clutters and detects aircraft signals. Based on many computer simulations, five heuristic strategies are presented: the Estimating Block and Filtering Block, Terrace Indication and Target Detection, Lattice Coefficient Map, Space Delay, and Initialization. In the test of stationary environment, we assign the high mountain and mild weather plus weak aircraft returns; in the test of nonstationary environment, the forested terrain and changing storm plus weak aircraft returns. The test results, outputs of the SBLP filter and pulse compressor, verify that the knowledge-based MTI can detect aircrafts well under SCR −50, −55 dB, and the heuristic strategies is effective to eliminate false alarms under the nonstationary condition.

Appendix Proof of Staggered Levinson-Durbin Relations (14) to (19)

Proof: Assuming that a stagger-period sequence $z(t_n)$, $n \in \{0, 1, \cdots\}$, is stationary, forward and backward transversal predictors and a lattice predictor, of order m (1 to M), at t_n, all operate with up to m+1 data of $\{(z(t_n)\}$ from low order to high order. When making one-step forward prediction of $z(t_n)$ with the last m data $z(t_{n-1})$, $z(t_{n-2})$, $\cdots$, $z(t_{n-m})$, the order m forward transversal predictor $\{h_m^f(t_n, \tau_j^f)\}$, $j \in \{0, 1, \cdots, m\}$, $m \in \{1, 2, \cdots, n\}$, $n \in \{1, 2, \cdots, M\}$, as shown in Figure 4, produces the prediction error

$$e_m^f(t_n) = \sum_{j=0}^{m} h_m^f(t_n, \tau_j^f) z(t_{n-j}),\ \tau_j^f = t_n - t_{n-j}, \quad (A1)$$

where $h_m^f(t_n, \tau_0^f)=1$. When making one-step backward prediction of $z(t_{n-m})$ with the first m data $z(t_{n-m+1})$, z

(t_{n-m+2}), ⋯, z (t_n), the order m backward transversal predictor $\{h_m^{b*}(t_n, \tau_j^b)\}$, $j \in \{0, 1, \cdots, m\}$, $m \in \{1, 2, \cdots, n\}$, $n \in \{1, 2, \cdots, M\}$, as shown in Figure 5, produces the prediction error

$$e_m^b(t_n) = \sum_{j=0}^{m} h_m^{b*}(t_n, \tau_j^b) z\,(t_{n+j-m}),\ \tau_j^b = t_{n+j-m} - t_{n-m}, \quad (A2)$$

where $h_m^b(t_n, \tau_0^b)=1$. From the formulas of staggered lattice predictor operation, (7) to (9) or Figure 3, we know that the forward and backward prediction errors of the stage m at the time t_n are a linear combination of the data z (t_{n-m}), z(t_{n-m+1}), ⋯, z (t_n). When substituting (A1) and (A2) into (7) to (9), we obtain that

$$\sum_{j=0}^{m} h_m^f(t_n, \tau_j^f) z\,(t_{n-j}) = \sum_{j=0}^{m-1} h_{m-1}^f(t_n, \tau_j^f) z\,(t_{n-j}) + R_m^f(t_n) \sum_{j=0}^{m-1} h_{m-1}^{b*}(t_{n-1}, \tau_j^b) z\,(t_{n+j-m}), \quad (A3)$$

and

$$\sum_{j=0}^{m} h_m^{b*}(t_n, \tau_j^b) z\,(t_{n+j-m}) = \sum_{j=0}^{m-1} h_{m-1}^{b*}(t_{n-1}, \tau_j^b) z\,(t_{n+j-m}) + R_m^b(t_n) \sum_{j=0}^{m-1} h_{m-1}^f(t_n, \tau_j^f) z\,(t_{n-j}). \quad (A4)$$

Comparing the coefficients of two sides of (A3), containing z (t_n), we have

$$h_m^f(t_n, \tau_0^f) = h_{m-1}^f(t_n, \tau_0^f) = 1,\ m \in \{1, 2, \cdots, n\},\ n \in \{1, 2, \cdots, M\}, \quad (A5)$$

and comparing the coefficients of two sides of (A4), containing z (t_{n-m}), we have

$$h_m^{b*}(t_n, \tau_0^b) = h_{m-1}^{b*}(t_{n-1}, \tau_0^b) = 1,\ m \in \{1, 2, \cdots, n\},\ n \in \{1, 2, \cdots, M\}. \quad (A6)$$

Comparing the coefficients of two sides of (A3), containing z (t_{n-m}), and in terms of (A6), we have

$$h_m^f(t_n, \tau_m^f) = R_m^f(t_n),\ m \in \{1, 2, \cdots, n\},\ n \in \{1, 2, \cdots, M\}, \quad (A7)$$

and comparing the coefficients of two sides of (A4), containing z (t_n), and in terms of (A5), we have

$$h_m^{b*}(t_n, \tau_m^b) = R_m^b(t_n),\ m \in \{1, 2, \cdots, n\},\ n \in \{1, 2, \cdots, M\}. \quad (A8)$$

Comparing the coefficients of two sides of (A3), containing z (t_{n-k}), $k \in \{1, 2, \cdots, m-1\}$, we have

$$h_m^f(t_n, \tau_k^f) = h_{m-1}^f(t_n, \tau_k^f) + R_m^f(t_n)\, h_{m-1}^{b*}(t_{n-1}, \tau_{m-k}^b),\ m \in \{2, 3, \cdots, n\},\ n \in \{2, 3, \cdots, M\}, \quad (A9)$$

and comparing the coefficients of two sides of (A4), containing z (t_{n+k-m}), $k \in \{1, 2, \cdots, m-1\}$, we have

$$h_m^{b*}(t_n, \tau_k^b) = h_{m-1}^{b*}(t_{n-1}, \tau_k^b) + R_m^b(t_n)\, h_{m-1}^f(t_n, \tau_{m-k}^f),\ m \in \{2, 3, \cdots, n\},\ n \in \{2, 3, \cdots, M\} \quad (A10)$$

(A7) and (A8) are (14) and (15), respectively, they are also (16) and (17); (A9) and (A10) are (18) and (19), respectively, i.e., the staggered L-D recursion relations hold.

References

[1] Simon Haykin. (2014). Adaptive Filter Theory, Fifth Edition. © Pearson Education Limited,. Edinburgh Gate, London, 110-114, 636-645, 785-790.

[2] Hanoch Lev-Ari, Thomas Kailath, and John Cioffi. (1984). Least-squares adaptive lattice and transversal filters: a unified geometric theory. IEEE Transactions on Information Theory, 30 (2), 222-236.

[3] Takafumi Takemoto, Naoto Sasaoka, Kensaku Fujii, and Yoshio Itoh. (2010). Speech enhancement system based on lattice filter and system identification. 10th International Symposium on Communications and Information Technologies, 441-446, doi: 10.1109/ISCIT.2010.5664880.

[4] Gediminas Simkus, Martin Holters, and Udo Zolzer. (2013). Ultra-low latency audio coding based on DPCM and block companding. 14th International Workshop on WIAMIS, Paris, 1-4, doi: 10.1109/WIAMIS.2013.6616143.

[5] Kensaku Fujii, Masaaki Tanaka, Naoto Sasaoka, and Yoshio Itoh. (2007). Method estimating reflection coefficients of Adaptive lattice filter and its application to system identification. The Acoustical Society of Japan, Acoust. Sci. & Tech. 28 (2), 98-104.

[6] Rui Zhu, Feiran Yang, and Jun Yang. (2016). A gradient-adaptive lattice-based complex adaptive notch filter. EURASIP Journal on Advances in Signal Processing, 2016: 79, 1-11, doi: 10.1186/s13634-016-0377-4.

[7] B. M. Keel and E. G. Baxa. (1990). Adaptive least square complex lattice clutter rejection filters applied to the radar detection of low altitude windshear. International Conference on ASSP, 1496-1472, doi: 10.1109/ICASSP.1990.115677.

[8] Dmitri N. Moisseev, Cuong M. Nguyen, and V. Chandrasekar. (2008). Clutter suppression for staggered PRT waveforms. J. Atmos. Oceanic Technol. 25, 2209-2218. doi: 10.1175/2008JTECHA1096.1.

[9] John Y. N. Cho and Edward S. Chornoboy. (2005). Multi PRI signal processing for the terminal Doppler weather radar. Part I: Clutter filtering. J. Atmos. Oceanic Technol. 22, 575-582.

[10] Andrzej Wojtkiewicz and Michal Tuszynski. (1992). Application of the Dirichlet transform in analysis of nonuniformly sampled signals. Proc. ICASSP. v25-v28.

[11] Xubao Zhang. (2017). Fourier analyses of stagger-period sequences. IJRDO-Journal of Electrical and Electronics Engineering, 3 (9), 1-12.

[12] S. Haykin, B. W. Currie, and S. B. Kesler. (1982). Maximum-entropy spectral analysis of radar clutter. Proceedings of the IEEE, 70 (9), 953-962. doi: 10.1109/PROC.1982.12426.

[13] Zhang Xubao. (2021). Finite impulse response filters for stagger-period signals, their designs and applications. European Journal of Information Technologies and Computer Science 1 (1), 1-11. doi: http://dx.doi.org/10.24018/compute.2021.1.1.3.

[14] J. Makhoul. (1977). Stable and efficient lattice methods for linear prediction. IEEE Trans. on ASSP, 25 (5), 423-428.

[15] C. J. Gibson and S. Haykin. (1980). Learning characteristics of adaptive lattice filtering algorithms. IEEE Trans. ASSP, 28 (6), 681-691.

[16] Rohit Negi and P G Poonacha. (1998). Convergence and bias in the LSG algorithm for adaptive lattice filters. Sadhana in India, 23, Part l, 83-91.

[17] Michael L. Honig and David G. Messerschmitt. (1981). Convergence properties of an adaptive digital lattice filter. IEEE Transactions on ASSP, 29 (3), 642-653.

[18] R. J. Wang. (1972). Optimum window length for the measurement of time-varying power spectra. The J. of Acoustical Society of America, 52 (1), 33-38.

[19] Tian-You Yu, R. Reinoso-Rondinel, and R. D. Palmer. (2008). A new way to investigate dynamics in a storm using doppler spectra from weather radar. 24th Int. Conf. on Interactive Information and Processing Systems (IIPS) for Meteorology, Oceanography, and Hydrology at New Orleans, 6B9: 1-8.

[20] Lai, Y.-C. and Baxa, E. G. Jr. (1993). On the application of the LMS-based adaptive noise canceller in nonstationary environment associated with airborne Doppler weather radar. IEEE International Conference on Acoustics, Speech, and Signal Processing, III: 25-28.

Biography

Xubao Zhang received his doctorate in Electronics from Xi'an Electronic Science and Technology University in China in 1989, and was a Postdoctoral Fellow at McMaster University in Canada in 1993. He has been interested in radar signal processing study and hearing aid technology research.

He worked as Associate Professor at electronic engineering department of Xi'an Electronic Science and Technology University. And he worked as an Electroacoustic and EMC engineer with Unitron Hearing.

He is the author of one book and more than 50 articles. He received an award: The Second-Prize of Science and Technology Progress 1992, in China.